β2M Signals Monocytes Through Non-Canonical TGFβ Receptor Signal Transduction

Zachary T. Hilt[1,2], Preeti Maurya[1], Laura Tesoro[1,3], Daphne N. Pariser[1], Sara K. Ture[1], Simon J. Cleary[4], Mark R. Looney MR[4], Kathleen E. McGrath[5], Craig N. Morrell[1]*

[1]Aab Cardiovascular Research Institute, University of Rochester School of Medicine, Rochester, New York, USA;[2]Department of Microbiology and Immunology, Cornell University, Ithaca, NY, USA; [3]Cardiology Department, University Francisco de Vitoria/Hospital Ramón y Cajal Research Unit (IRYCIS), CIBERCV, 28223 Madrid, Spain; [4]Department of Medicine, UCSF, San Francisco, United States of America[5]Center for Pediatric Biomedical Research, Department of Pediatrics, University of ; Rochester School of Medicine, Rochester, New York, USA.

Running title: β2M Promotes Monocyte TGFβR Non-Canonical Pathway

Subject Terms:
Cell Signaling/Signal Transduction
Growth Factors/Cytokines
Inflammation
Pathophysiology
Vascular Biology

***Address correspondence to:**
Dr. Craig Morrell
Aab Cardiovascular Research Institute, Box CVRI
601 Elmwood Avenue
Rochester, NY 14642
Craig_Morrell@URMC.Rochester.edu

This manuscript was sent to Francesco Violi, Consulting Editor, for review by expert referees, editorial decision, and final disposition.

ABSTRACT

***Rationale*:** Circulating monocytes can have pro-inflammatory or pro-reparative phenotypes. The endogenous signaling molecules and pathways that regulate monocyte polarization *in vivo* are poorly understood. We have shown that platelet derived beta-2 microglobulin (β2M) and transforming growth factor beta (TGFβ) have opposing effects on monocytes by inducing inflammatory and reparative phenotypes respectively, but each bind and signal through the same receptor. We now define the signaling pathways involved.

***Objective*:** To determine the molecular mechanisms and signal transduction pathways by which β2M and TGFβ regulate monocyte responses both *in vitro* and *in vivo*.

***Methods and Results*:** Wild-type (WT) and platelet specific β2M knockout (Plt-β2M$^{-/-}$) mice were treated intravenously with either β2M or TGFβ to increase plasma concentrations to those in cardiovascular diseases. Elevated plasma β2M increased pro-inflammatory monocytes, while increased plasma TGFβ increased pro-reparative monocytes. TGFβ receptor (TGFβR) inhibition blunted monocyte responses to both β2M and TGFβ *in vivo*. Using imaging flow cytometry, we found that β2M decreased monocyte SMAD2/3 nuclear localization, while TGFβ promoted SMAD nuclear translocation, but decreased non-canonical/inflammatory (JNK and NFκB nuclear localization). This was confirmed *in vitro* using both imaging flow cytometry and immunoblots. β2M, but not TGFβ, promoted ubiquitination of SMAD3 and SMAD4, that inhibited their nuclear trafficking. Inhibition of ubiquitin ligase activity blocked non-canonical SMAD-independent monocyte signaling and skewed monocytes towards a pro-reparative monocyte response.

***Conclusions*:** Our findings indicate that elevated plasma β2M and TGFβ dichotomously polarize monocytes. Furthermore, these immune molecules share a common receptor, but induce SMAD-dependent canonical signaling (TGFβ) versus non-canonical SMAD-independent signaling (β2M) in a ubiquitin ligase dependent manner. This work has broad implications as β2M is increased in several inflammatory conditions, while TGFβ is increased in fibrotic diseases.

Keywords:
Cell signaling, cytokine, inflammation, platelet, monocyte.

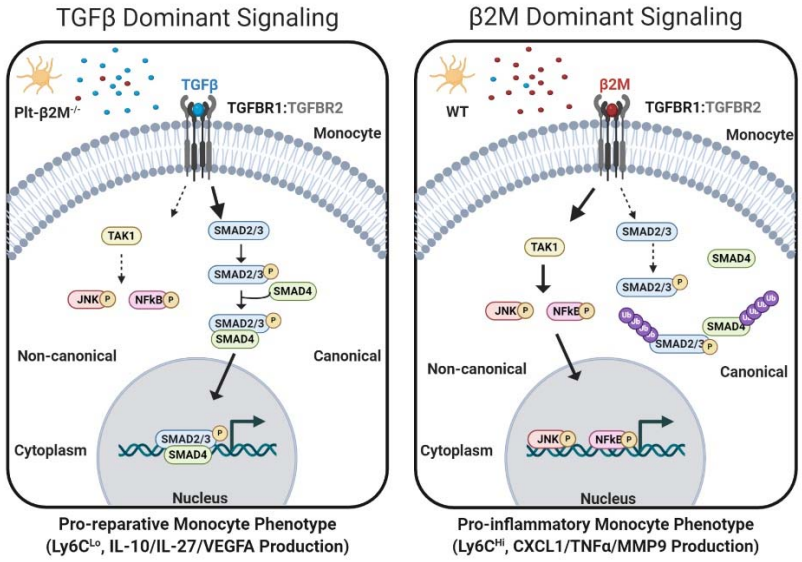

Nonstandard Abbreviations and Acronyms:

β2M	Beta-2 microglobulin
ELISA	Enzyme-linked immunosorbent assay
TGFβ	Transforming growth factor beta
TGFβR	Transforming growth factor beta receptor
IL	Interleukin
qRT-PCR	Quantitative real-time polymerase chain reaction

INTRODUCTION

Monocytes are bone marrow derived innate immune cells that circulate for about 2 days before being cleared from the circulation. Circulating monocytes scan for pathogens and respond to inflammatory signals needed to perform their phagocytic functions, or monocytes can tissue migrate to become macrophages. Monocytes are not a uniform cell population; there is significant monocyte heterogeneity determined by the immune environment. In mice, monocytes are typically classified as either pro-inflammatory ($Ly6C^{Hi}$) or pro-reparative ($Ly6C^{Lo}$). $Ly6C^{Hi}$ monocytes are functionally characterized by their antimicrobial activity, release of reactive oxygen species (ROS), and by the secretion of cytokines such as TNF-α, Cxcl1/KC and IL-1β[1, 2]. $Ly6C^{Lo}$ monocytes release pro-reparative cytokines such as IL-10, IL-27, and pro-angiogenic and tissue repair factors such as VEGF[3, 4]. Monocyte phenotypes are plastic, as $Ly6C^{Lo}$ monocytes can arise from pre-existing $Ly6C^{Hi}$ monocytes. Human monocytes are typically divided into classical ($CD14^{++}CD16^{-}$), intermediate ($CD14^{++}CD16^{+}$), and non-classical ($CD14^{+}CD16^{++}$). Human classical monocytes are phagocytic, ROS producing, and release high levels of the pro-reparative cytokine IL-10[5-7]. Intermediate human monocytes are functionally defined as having a pro-inflammatory cytokine profile[6, 7] and upregulate genes related MHC II processing and presentation[6, 7]. Non-classical monocytes are functionally defined by their patrolling behavior, granzyme production, and pro-inflammatory cytokine production upon TLR stimulation[6, 7] and upregulating Fc receptor mediated phagocytosis[7].

Much of our understanding of monocyte polarization comes from *in vitro* studies. Immune mediators such as LPS, IFN-γ, and GM-CSF induce "pro-inflammatory" monocyte polarization that are M1-like inflammatory macrophages upon tissue trafficking[8-10]. Conversely, IL-4, IL-13, IL-10, TGF-β1, M-CSF induce pro-reparative monocyte and macrophage polarization[8, 9, 11]. We previously demonstrated that platelet derived beta-2 microglobulin (β2M) induced an inflammatory monocyte phenotype[12, 13], and now expand our findings to demonstrate that monocyte phenotype and polarization is in part driven by plasma β2M and TGFβ ratios *in vivo.* Platelets are the major plasma source of both β2M and TGFβ and platelet derived β2M inflammatory phenotype is opposed by TGFβ[12]. Furthermore, we discovered that β2M binds to the transforming growth factor beta receptor (TGFβR) and induces, a monocyte inflammatory phenotype[12]. We now demonstrate the downstream signaling mechanisms that in part account for how these β2M and TGFβ bind the same receptor complex, but mediate different downstream monocyte phenotype outcomes.

TGFβR downstream signaling is mediated through either canonical or non-canonical pathways. Canonical signaling occurs when a ligand binds TGFβR2, TGFβR1 is recruited, a heterodimer is formed, and TGFβR1is phosphorylated. TGFβR1 phosphorylation leads to the recruitment of SMAD2 and SMAD3, which in-turn become phosphorylated,[14] and SMAD4 is recruited to form a complex that translocates to the nucleus to act as a transcription factor[15]. The canonical pathway primarily leads to a reparative monocyte phenotype[11]. Non-canonical TGFβR signaling involves SMAD-independent molecules such as AKT, ERK, P38, JNK, and NFκB. Ligand stimulation of the TGFβR complex triggers TRAF6 and/or E3 ubiquitin ligase activation that allows for TAK1 ubiquitination and its activation[16, 17]. TAK1 is upstream of both JNK

and NFκB making it indispensable for non-canonical pathway signaling [16, 18]. Ubiquitinated TAK1 is activated, leading to the activation of JNK and NFκB proteins and their nuclear translocation, resulting in pro-inflammatory gene expression and monocyte/macrophage polarization[19, 20]. Ubiquitin is therefore a central regulator of the TGFβR signal transduction pathway. SMAD ubiquitination by E3 ubiquitin ligases prevents both its nuclear translocation and its DNA binding[21-23]. Conversely, non-canonical signaling requires ubiquitin ligase activity for the activation of TAK1 and downstream inflammatory pathways.

We now present data demonstrating that plasma β2M signals monocytes through a TGFβR dependent, non-canonical signal transduction pathway. These data provide novel insights into the regulation of monocyte polarization.

METHODS

The data that support the findings of this study are available from the corresponding author upon reasonable request.

More detailed methods can be found in Material in the Data Supplement.

Please see the Major Resources Table in Material in the Data Supplement.

Mouse studies.

All mice used in these experiments were on a C57BL6/J background. Mice were between 4 and 8 weeks old at the time of experiment to study age independent effects, as we have shown age influences monocyte phenotype[13]. Male and female mice were used in our experiments as we have previously shown no difference between genders in our mouse model[12]. Mice were randomly assigned to either control or treatment by cage and were kept in the same cage after treatment assignment. Mice were euthanized and all samples collected, prepared, and analyzed independent of each other using the same methods within a study group. In this way each animal was treated as treatment independent.

Group size of animals were determined from previously performed experiments under similar conditions[12, 13]. Wild-type mice were obtained from Jackson Laboratory (000664) and the generation of PF4Cre-β2M$^{Flox/Flox}$ mouse line has been previously described[12].

To obtain whole blood, mice were bled retro-orbital into EDTA blood collection tubes (Greiner Bio-One). Mouse platelets were obtained by retro-orbital bleed into heparinized Tyrodes solution. Detailed protocol of how the blood was processed can be found in Data Supplement.

Mice were injected with PBS, recombinant human β2M (5 µg, BD Bioscience, BD551089) or recombinant mouse TGFβ1 (20 ng, ProSpec, CYT-858) by intravenous (I.V.) injections in 100 µL dilution each day for 3 days. Mice were bled before the first injection (D0) and then on D4. For SB431542 (EMD Milipore Calbiochem, 616461) inhibitor experiments, mice were injected with: DMSO (7%) as vehicle control, 175 µg/kg/mouse of SB431542 in DMSO, 250 µg/kg/mouse of β2M, 1 µg/kg/mouse of TGFβ ± SB431542. Endotoxin levels of β2M, TGFβ1 and LPS were measured by Pierce™ LAL Chromogenic Endotoxin Quantitation Kit (Thermo Fisher Scientific, 88282).

For biodistribution experiments mice were injected with 5 µg of β2M or 20 ng of TGFβ I.V., then 24 hours later bone marrow, liver and spleen were harvested. Processing of the bone marrow, liver and spleen are detailed in Data Supplement.

All mouse work conducted in this study was approved by the University of Rochester Institutional Animal Care and Use Committee under protocol number 2009-022.

Enzyme-Linked Immunosorbent Assay.
Human IL-8 (R&D Systems, DY20805) was measured by ELISA from THP-1 supernatant. Mouse plasma TGFβ1 was measured by ELISA (R&D systems, DB100B). Mouse plasma β2M was measured by ELISA (Aviva System, OKEH00344). Details outlining how the ELISA was performed are provided in the Data Supplement.

Absorbance was collected on FLUOstar OPTIMA by BMG LABTECH. ELISAs were analyzed using four parameter logistic curve-fit.

Flow Cytometry.
For flow cytometry, whole blood was diluted 1:20 into PBS, stained with antibodies for 30 mins and fixed with BD FACS Lysing Solution (BD Biosciences, 349202). Gating strategies are found in Data Supplement. All flow cytometry was acquired on either an Accuri C6 or BD LSR II. Collected flow cytometry data was analyzed on FlowJo version 10. Statistics for normality and significance was performed on GraphPad Prism Version 9.

Flow cytometry antibodies used can be found in Major Resource Table.

Imaging Flow Cytometry.
For ImageStream analysis whole blood was surface stained as for standard flow cytometry, washed with PBS, resuspended in 500 µL of Flow Cytometry Fixation Buffer (FC007, R&D Systems) at 4°C for 30 mins, vortexing intermittently. Cells were resuspended into 200 µL of Flow Cytometry Permeabilization/Wash Buffer (FC005, R&D Systems) and stained with intracellular antibodies (pJNK, pSMAD2/3, NFκB, NR4A1, SMAD4) for 30 mins at 4°C. Excess antibody was washed with 1 mL of Flow Cytometry Permeabilization/Wash Buffer and then resuspended into 60 µL of PBS. ImageStream was collected on the Amnis ImageStream GenX. IDEAS 6.2 software was used to compensate and analyze ImageStream data.

Antibodies used can be found in Major Resource Table.

Cell Culture.
THP-1 cells (ATCC) were incubated in RPMI media supplemented with 1x glutamax (Thermo Fisher Scientific), 2% penicillin/streptomycin (Invitrogen), 10% fetal bovine serum (FBS), 1X sodium pyruvate, 1X essential medium vitamins, 1X non-essential amino acids (Life Technologies). Primary mouse monocytes were isolated by flushing femur and tibia bone marrow using isolation buffer (1X PBS, 2% FBS, 1mM EDTA, Gibco) and a 20-gauge needle (BD Bioscience). RBC were lysed with ACK lysis buffer (Gibco). RAW 264.7 macrophages (ATCC) and primary mouse monocytes were cu in DMEM media supplemented with same as RPMI media listed earlier. Cells were pre-treated with 10 µM of inhibitor Heclin 30 mins prior to agonist. Recombinant proteins were used to treat cells at concentrations of 5 µg/mL for β2M,10 ng/mL recombinant human TGFβ (ProSpec, L6529), 10 ng/mL LPS (Sigma Aldrich, L6529), and/or Polymyxin B (Cayman Chemical, 14157) at 0, 1, 3, 6, 12, 24, 48 hrs. For cells treated with platelet releasate, anti-β2M antibody (BioXCell, BE0143, 10 µg/mL) or anti-TGFβ (BioXCell, BE0057, 1 µg/mL) was incubated for 1 hr prior to treatment with platelet releasate. THP-1s were phenotypically defined by CD14 and CD16 expression. Intracellular proteins were stained and analyzed for nuclear localization as described above. Release of cytokines in the supernatant were analyzed by ELISA. Transcript levels were analyzed by qRT-PCR.

Immunofluorescence staining and confocal imaging.
THP-1 cells were cultured on poly-L-lysin coated glass chamber slides and treated with recombinant β2M (5 μg/mL) or TGFβ1 (10 ng/mL) for 3, 6 and 12 hrs. Detailed instructions on how cells were stained for imaging can be found in Data Supplement. Images were acquired for SMAD4, pJNK and DAPI staining using Olympus FV1000 confocal laser scanning microscope using a 60x oil-immersion objective lens with 4x electronic zoom and image resolution size was 1024x1024[24].

Monocyte Isolation.
Primary mouse monocytes from whole blood were isolated using EasySep™ Mouse Monocytes Isolation Kit (STEMCELL Technologies, 19861), following manufacturers guidelines. Isolated mouse monocytes were resuspended into RLT lysis buffer and RNA was isolated following the instructions of RNeasy Mini Kit (Qiagen, 74106).

Quantitative real-time polymerase chain reaction.
RNA was obtained from primary mouse monocytes (whole blood and bone marrow derived) and cell lines (THP-1, RAW 264.7) using RNeasy Mini Kit. Concentration of all isolated mRNA was measured using NanoDrop™ 2000 (Thermo Fisher Scientific). Isolated mRNA was converted into cDNA using High Capacity RNA-to-cDNA kit (Applied Biosystems, 4387406). Gene expression was measured using TaqMan gene expression master mix (Thermo Fisher Scientific, 4369016) on the BioRad iCycler IQ5 (1708740). Gene expression of qRT-PCR was analyzed in Microsoft Excel using calculation for fold change $2^{(-\text{delta delta CT})}$ with housekeeping genes of GAPDH for mice or 18S ribosome for humans and normalized to control samples. The amplification condition consisted of an initial polymerase activation at 95 °C for 10 min followed by amplification of the target cDNA for 40 cycles (denature at 95°C for 15 sec, anneal/extend at 60°C for 1 min). All sample volumes were kept consistent at 20 uL per reaction. If no cycle threshold (Ct) value was observed after 40 cycles of amplification then graphs were labeled with not detectable (N.D.).

Primers used for qRT-PCR can be found in the Major Resource Table.

Cellular Fractionation.
Separation of the nuclear and cytoplasmic cellular fractions was conducted following Rockland Antibodies & Assays protocol. Cytoplasmic Extract (CE) buffer was prepared with 10 mM HEPES, 60 mM KCl, 1 mM EDTA, 1 mM DTT, 1 mM PMSF ± 0.075% (v/v) NP-40 at a pH of 7.6. Nuclear Extract (NE) buffer was made of 20 mM Tris Cl, 420 mM NaCl, 1.5 mM $MgCl_2$, 0.2 mM EDTA, 1 mM PMSF and 25% (v/v) glycerol at a pH of 8.0. Isolated cells were washed with PBS and centrifuged at 100 rcf, cells were resuspended in 100 μL of CE buffer and incubated on ice for 3 mins. Cells were spun at 100 rcf for 4 mins. The CE was isolated and put into a fresh tube, spun at max speed for 10 mins at 4ºC and then 20% glycerol was added and froze at -80ºC. The remaining cellular nuclei was washed with 100 μL of CE buffer without NP40 then spun at 100 rcf for 4 mins. The nuclear pellet was resuspended with 50 μL of NE buffer and 35 μL of 5 M NaCl. Another 50 μL of NE buffer was added to the pellet and incubated on ice for 10 mins, vortexing intermittently. The NE was centrifuged at max speed for 10 mins, decanted into a new tube and stored at -80ºC. Fractionated samples were resuspended into 2x Laemmli buffer for immunoblot.

Immunoprecipitation.
SMAD3 or SMAD4 were immunoprecipitated following immunoprecipitation kit directions (abcam, ab206996). Cells in suspension were collected by centrifugation and adherent cells were detached with Accutase. Washed cells were resuspended into lysis buffer, put on ice for 1 min and then mixed for 30 mins at 4ºC. Cells were centrifuged at 10,000g for 10 mins at 4ºC and transferred into a fresh tube. For antibody binding, 5 μL of SMAD3 and SMAD4 antibodies were added to 500 μL of sample in lysis buffer with protease inhibitor cocktail. Sample with antibody was mixed overnight at 4ºC. 25 μL/sample of Protein A/G Sepharose® was washed twice with 1 mL of wash buffer, centrifuging at 2000g for 2 mins.

After washes the Protein A/G Beads were suspended as 50% slurry in wash buffer. For bead capture, 25 µL of Protein A/G Sepharose® bead slurry was added to each tube of antibody/sample mixture for 1 hour at 4ºC. Sample was collected by centrifuging at 2000g for 2 mins at 4ºC. Samples were washed 3 times with 1 mL of wash buffer, centrifuging between. To elute samples 40 µL of 2x Laemmli buffer was added to the bead/sample mixture, boiled for 5 mins and centrifuged to elute. Samples were saved at -80ºC for immunoblotting.

Immunoblot.
Fractionated, immunoprecipitated, and organ samples in Laemmli buffer were loaded into Mini-PROTEAN® TGX Gels (BioRad). The loaded gels were run at 100V in 1X Tris/Glycine/SDS buffer. Transfer from the SDS-PAGE gel to nitrocellulose membrane (BioRad) was conducted at 110V for 1 hr with ice packs. Transferred blots were blocked in 3% BSA (Sigma Aldrich) in tris-buffered saline (TBS, Fisher Scientific) with 0.1% Tween-20 (TBS-T) for 1 hr, shaking at room temperature. Primary antibodies (SMAD3, SMAD4, NFκB, TBP, GAPDH, Ubiquitin) were diluted 1:1000 in blocking buffer and incubated overnight at 4ºC. Anti-rabbit or -mouse HRP was used as secondary antibody (GE Healthcare) and diluted 1:1000 in 5% milk for 1 hours at room temperature with gentle agitation. Incubated membranes were developed using Supersignal West Pico (Thermo Fisher) using BioRad ChemiDoc MP chemiluminescence setting.

Antibodies for immunoblot can be found in the Major Resource Table.

Statistical analysis.
All experiments are representative and repeated at least twice. All statistical tests were conducted using GraphPad Prism Version 9.0.0. A Shapiro-Wilk test for normality was performed on the data. For data sets that passed normality test and contained more than two independent groups, one-way ANOVA was used with a Bonferroni's multiple comparison correction test. If the data set did not pass normality then a Kruskal-Wallis test with Dunn's multiple comparisons correction was performed. P-values of <0.05 were considered statistically significant and represented on graph by 1 star. All P-values <0.01 were graphically represented by 2 stars. All data was graphed as mean ± standard error of the mean (SEM) or standard deviation (SD) where indicated in the figure legends.

RESULTS

Increased plasma β2M and risk of major adverse cardiac events are directly correlated.[25] We previously showed that β2M signaled monocytes at concentrations >2 µg/mL *in vitro,* a concentration found in many cardiovascular diseases, including in patients immediately post-myocardial infarction[12]. To directly determine whether an increase in plasma β2M leads to an inflammatory monocyte phenotype, we injected wild-type (WT) C57BL/6 mice and platelet-specific $\beta2M^{-/-}$ mice ($PF4Cre\text{-}\beta2M^{Flox/Flox}$ mice, Plt-$\beta2M^{-/-}$) with 5 µg of recombinant β2M intravenously (i.v.) each day for 3 days. On D4 plasma β2M concentrations were confirmed to be elevated with no significant change in TGFβ (Online supplementary data Fig IA). WT mice had a higher percentage of $Ly6C^{Hi}$ monocytes on D0 compared to Plt-$\beta2M^{-/-}$ mice (Figure 1A, left panel). On D4 there was a significant increase in the percentage of circulating pro-inflammatory $Ly6C^{Hi}$ monocytes in both β2M treated WT and Plt-$\beta2M^{-/-}$ mice, indicating that β2M may directly induce a $Ly6C^{Hi}$ phenotype (Figure 1A). β2M injections led to the expression of the pro-inflammatory cytokine *Cxcl1* mRNA in both WT and Plt-$\beta2M^{-/-}$ mouse monocytes (Figure 1A, right panel). However, monocytes from WT mice on D4 post-injection had higher *Cxcl1* expression compared to Plt-$\beta2M^{-/-}$ (Fig 1A). β2M injections did not change the total number of circulating mature B cells, $CD4^+$ or $CD8^+$ T cells (Online Figure IB-D). However, there was an increase in total neutrophils post-β2M injection in both WT and Plt-$\beta2M^{-/-}$ mice (Online Figure IE). To further phenotype circulating monocytes, the

expression of mRNA indicative of a reparative phenotype including *Il27, Il10* and *Nr4a1* was higher basally in Plt-β2M$^{-/-}$ mice compared to WT mice (Figure 1B), and after β2M injections the expression of each reparative marker was decreased or not detectable in both WT and Plt-β2M$^{-/-}$ mice (Figure 1B). Recombinant β2M and TGFβ were confirmed to have minute concentrations of endotoxin at the concentrations used in animals (Online Figure IIA). We also confirmed the presence of detectable levels of β2M in the bone marrow and spleen, but not the liver (Online Figure IIB) after *in vivo* injection, demonstrating a hematopoietic tissue distribution. TGFβ was not higher in the bone marrow, spleen or liver post-injection, demonstrating it largely stayed in the circulation (Online Figure IIB). Together, these data suggest that platelet β2M promotes an inflammatory monocyte polarization *in vivo*.

We previously found that β2M induced SMAD3 phosphorylation despite an inflammatory phenotype[12], but SMAD3 must translocate to the nucleus to act as a transcription factor. To determine whether β2M altered SMAD trafficking *in vivo*, we performed imaging flow cytometry. Blood was isolated on D0 and D4 after daily β2M injections and blood monocytes were identified by Ly6C staining. Intracellular DAPI staining was used to identify nuclear versus cytoplasmic localization of phosphorylated SMAD2/3 (pSMAD2/3). There was greater circulating monocyte nuclear pSMAD2/3 in Plt-β2M$^{-/-}$ compared to WT mice at baseline (Figure 1C). On D4 nuclear localization of pSMAD2/3 was greatly decreased compared D0 in both WT and Plt-β2M$^{-/-}$ mice (Figure 1C). These data suggest that despite SMAD phosphorylation, β2M signaling limits SMAD nuclear trafficking *in vivo*.

Because our prior studies demonstrated β2M and TGFβ antagonistically modulated monocyte polarization, we next determined the effects of elevated plasma TGFβ on monocyte differentiation. Mice were injected i.v. with 20 ng of recombinant TGFβ each day, for 3 days. Mice were bled on D0 before injections, and again on D4 after injections. Plasma TGFβ was increased, and plasma β2M unchanged, on D4 (Online data Fig IIIA). Similar to Figure 1, WT and Plt-β2M$^{-/-}$ mice had a difference in the percentage of Ly6C^{Hi} monocytes pre-TGFβ (Figure 2A), but TGFβ treatment decreased the percentage of Ly6C^{Hi} monocytes in WT mice (Figure 2A). No change in the total number of circulating neutrophils, CD4, or CD8 T cells were observed on D4 post-TGFβ injections (Online Figure IIIC-E). However, there was a significant decrease in circulating mature B cells in WT mice after injections (Online Figure IIIB). Isolated circulating monocytes were analyzed for immune related transcripts using qRT-PCR. Reparative monocyte markers *Arg1, Chil3* and *Vegfa* were significantly upregulated in both WT and Plt-β2M$^{-/-}$ monocytes on D4 post-injections (Figure 2B). *Il10* was increased in monocytes from Plt-β2M$^{-/-}$ mice compared to WT monocytes on D0, but post-injection *Il10* was significantly increased in WT mouse monocytes compared to both WT baseline and D4 Plt-β2M$^{-/-}$ mouse monocytes (Figure 2B). Plasma KC, an inflammatory monocyte cytokine, was measured by ELISA on D0 and D4 in mice treated with either β2M or TGFβ. β2M increased plasma KC in both WT and Plt-β2M$^{-/-}$ mice (Figure 2C), but TGFβ did not change plasma KC (Figure 2C). These data further indicate that β2M and TGFβ drive different monocyte phenotypes *in vivo*.

Imaging flow cytometry was next employed to determine the effect of elevated plasma TGFβ on canonical and non-canonical TGFβR signaling. TGFβ increased both monocyte SMAD4 and NR4A1 nuclear localization in WT and Plt-β2M$^{-/-}$ mice (Figure 2D). In contrast, non-canonical signal transduction proteins, pJNK and NFκB, co-localization with DAPI were significantly decreased in WT monocytes compared to Plt-β2M$^{-/-}$ mouse monocytes on D0. TGFβ decreased nuclear pJNK in both WT and Plt-β2M$^{-/-}$ mice at D4 and nuclear NFκB only in WT mice (Figure 2E). These data suggest that elevated plasma TGFβ shifts TGFβR signal transduction towards a SMAD-dependent reparative monocyte phenotype, while β2M has the opposite effect.

Both β2M and TGFβ bind directly to, and signal through, the TGFβR and monocytes lacking TGFβR do not respond to either β2M or TGFβ[12]. To demonstrate that β2M and TGFβ downstream signal transduction is TGFβR dependent *in vivo*, WT mice were treated with the ALK5/TGFβRI inhibitor SB431542[26] and recombinant β2M or TGFβ as above. Recombinant β2M injection increased Ly6C^{Hi}

monocytes, that was attenuated by SB431542 treatment (Online Figure IVA and gating Online Figure VA). There was no significant difference in the total number of circulating $CD3^+$, $CD8^+$ or $CD4^+$ T cells or total monocytes after SB431542 (Online Figure IVB-E), but there was a decrease in neutrophils between TGFβ and SB431542 treatment groups compared to vehicle control (Online Figure IVF). Mature B cells were significantly increased by SB431542 and β2M treatment compared to β2M alone (Online Figure IVG). To phenotype circulating monocytes, we determined the expression of *Cxcl1* (inflammatory) and *Il27* (reparative) in isolated monocytes. As expected, β2M induced *Cxcl1* and TGFβ induced *Il27,* but each were blocked by TGFβR inhibitor (Figure 3A). Transcription factor trafficking *in vivo* was also determined using imaging flow cytometry. We observed an increase of surface Ly6C after β2M injections, that was decreased by SB431542 (Online Figure IVB). TGFβ, but not β2M, injections increased nuclear localization of SMAD4 and NR4A1 that was reduced by SB431542 (Figure 3B-C). Treatment with β2M and TGFβ increased nuclear pJNK *in vivo* that was partially attenuated by SB431542 (Fig 3D). These data indicate that *in vivo* inhibition of ALK5/TGFβRI kinase activity inhibited both β2M and TGFβ mediated monocyte polarization.

To further validate our *in vivo* findings and demonstrate direct signaling in a human monocyte cell line, THP-1 cells were treated with recombinant β2M and TGFβ for 0, 3, 6, 12, and 24 hrs and cellular fractionation preformed to isolate cytoplasmic and nuclear protein fractions. Each cell fraction was immunoblotted for NFκB as a non-canonical, and SMAD3 as a canonical, signaling protein marker. Nuclear fractions of β2M treated cells had increased NFκB 12- and 24-hrs post-treatment, while there was no NFκB nuclear localization with TGFβ treatment (Figure 4A). SMAD3 was not different in the cytoplasmic fractions following either β2M or TGFβ treatment (Figure 4B). TGFβ, but not β2M, induced total and pSMAD3 nuclear localization (Online Figure VIA). To confirm that THP-1 cells functionally respond to stimulation, we treated cells with LPS or LPS with Polymixin B to block the translocation of NFκB. LPS induced the translocation of NFκB into the nucleus as expected, which was reduced by Polymyxin B (Online Figure VIB). No change in SMAD3 nuclear localization was observed with LPS or LPS and Polymyxin B (Online Figure VIC).

As a complimentary means to assess β2M and TGFβ responses in primary cells, we performed imaging flow cytometry on primary mouse bone marrow monocytes treated with recombinant β2M or TGFβ for 0, 3, 6, 12, and 24 hrs. There was a significant increase in nuclear pJNK at 6 - 24 hrs post-β2M treatment while TGFβ decreased pJNK nuclear localization (Figure 4C). There was no significant difference in the nuclear localization of either pSMAD2/3 or SMAD4 when monocytes were treated with β2M (Figure 4D-E), but TGFβ increased the nuclear localization of pSMAD2/3 and SMAD4 early post-treatment compared to control (Figure 4D-E). To further validate our cellular fractionation and imaging flow cytometry data, we performed immunofluorescent staining and confocal imaging on THP-1 cells treated with β2M and TGFβ for 0, 3, 6 and 12 hrs. Inflammatory pJNK was observed in the nucleus of β2M treated cells, while TGFβ lead to both cytoplasmic and some nuclear staining that diminished over time (Figure 4F). SMAD4 was observed to accumulate in the cytoplasm of THP-1 cells after β2M treatment; conversely, TGFβ treated cells had SMAD4 nuclear localization (Figure 4G). Non-specific binding was not observed in cells stained with only secondary antibody (Online Figure VII).

To demonstrate β2M-dependent canonical vs non-canonical platelet mediated monocyte signaling, we treated monocytes with platelet releasate or releasate and anti-β2M antibody. Platelet releasate increased the nuclear translocation of pJNK and decreased pSMAD2/3 (Figure 4H). This was attenuated by anti-β2M antibody (Figure 4H). To determine the effects of platelet derived TGFβ, we performed imaging flow cytometry on monocytes treated with platelet releasate, or with releasate and anti-TGFβ antibody. Monocytes treated with platelet releasate and anti-TGFβ antibody had decreased pSMAD2/3 and increased pJNK nuclear localization compared to IgG control and platelet releasate with no antibody (Online Figure VIIIA-B). Platelets are not the only source of plasma β2M, although our PF4-Cre-$\beta2M^{Flox/Flox}$ mice indicated they are a dominant source[12]. To determine whether endothelial cells also contribute to plasma

β2M, we measured plasma β2M in endothelial specific $\beta2M^{-/-}$ mice (VE-Cadherin-Cre-$\beta2M^{Flox/Flox}$ / VE-Cad-Cre+). There was no significant difference in plasma levels of β2M or TGFβ in VE-Cad-Cre+ mice (Online Figure IXA-B). These data suggest that while most cells contain β2M, platelets are a dominant cellular source.

To explore how β2M and TGFβ driven transcription factor nuclear trafficking changes gene expression, THP-1 cells were treated with recombinant β2M or TGFβ for 0, 1, 3, 6 and 24 hrs and mRNA was collected for qRT-PCR. Recombinant β2M increased *Cxcl8* (peaking at 6 hrs) and *Tnf* (more sustained over the 48 hr time period) (Figure 4I). TGFβ also increased *Cxcl8*, however the peak and duration were much less than induced by β2M treatment (Figure 4I). Conversely, recombinant β2M did not increase the pro-reparative transcripts *Il10* and *Arg1*, while recombinant TGFβ increased each, starting as early as 1 hr post-treatment (Figure 4I). Because monocytes are important for tissue and extracellular matrix (ECM) remodeling, we analyzed transcripts for metalloproteinases (*Mmp9*) and tissue inhibitor of metalloproteinases (*Timp1*) that promotes ECM stability. β2M significantly increased *Mmp9*, peaking at about 6 hrs and stayed elevated, while TGFβ significantly increased *Timp1* starting at 1 hr, that peaked at 24 hrs (Figure 4I). Taken together, these data indicate that β2M and TGFβ differentially regulate monocyte transcription factor translocation and downstream transcripts; β2M promotes inflammatory transcripts, while TGFβ promotes reparative transcripts.

Ubiquitin is a regulator of TGFβR downstream signaling. The canonical pathway is inhibited by ubiquitination, while non-canonical signaling is dependent on E3 ubiquitin ligases[16, 17, 27, 28]. SMAD2, SMAD3 and SMAD4 ubiquitination inhibits their ability to act as a transcription factors by either sequestering SMADs to the cytoplasm, or leading to their proteasome-dependent degradation[21-23, 29, 30]. In contrast, non-canonical TRAF6-TAK1 signaling is ubiquitin ligase dependent. Because β2M and TGFβ differentially activated non-canonical and canonical signaling, but both function through the TGFβR, we hypothesized that this may in part be ubiquitin dependent. To explore this, THP-1 cells were treated with a E3 ubiquitin ligase inhibitor, Heclin (10 μM). Heclin inhibits HECT domain-containing E3 ubiquitin ligases related to canonical TGFβR signaling, including Nedd4, Smurf2 and WWP1[31 23, 29, 32]. THP-1 cells were pre-treated with either DMSO or Heclin for 30 mins, then treated with PBS, β2M or TGFβ for 24 hrs. THP-1 cells treated with β2M had increased surface CD16 indictive a non-classical monocyte phenotype, that was partially attenuated by Heclin (Figure 5A). We confirmed that blocking ubiquitin ligase activity was not cytotoxic as Heclin by itself or with ligand stimulation did not induce cell death as measured by 7AAD expression (Online Figure XA). However, TGFβ with or without Heclin slightly increased cell death (Online Figure XA). THP-1 cells treated with β2M had increased inflammatory associated transcripts *Tnf* and *Mmp9* and detectable levels of *Fcgr3a* (CD16), but each was blocked by ubiquitin ligase inhibitor (Figure 5B). Heclin treatment had no effect on TGFβ induced *Vegfa*, *Nr4a1*, and *Il10,* and increased *Il10* on its own (Figure 5B). There was no difference in the expression of transcription factors *Nfkb*, *Mapk8*, *Smad3* and *Smad4* upon ligand or Heclin treatment (Online Figure XB).

To demonstrate that Heclin is not a general inhibitor of monocyte inflammatory responses, we treated cells with LPS with and without Heclin, as LPS signaling is not ubiquitin ligase dependent[33]. LPS significantly increased surface CD16, even in the presence of Heclin (Online Figure XIA) and did not change LPS induced *Cxcl8* (Online Figure XIB). LPS treatment in presence of Heclin increased *Nr4a1, Mapk8* and decreased *Nfkb* (Online Figure XIB). These data suggest that inhibition of ubiquitin ligases blocks β2M, but not LPS mediated monocyte inflammatory responses.

To confirm that β2M and TGFβ differentially regulate SMAD ubiquitination, the murine macrophage cell line RAW 264.7 cells were treated with recombinant β2M or TGFβ for 0, 3, 6, 12, 24 and 48 hrs. Cells were collected at each time point, SMAD3 and SMAD4 were then immunoprecipitated and immunoblotted for ubiquitin. β2M, but not TGFβ, increased SMAD ubiquitination (Figure 6A, 6C, SMAD3 quantification Online Figure XIIB). As a control, RAW 264.7 macrophages were treated with

LPS or LPS with Polymyxin B and SMAD3 immunoprecipitated. No difference in SMAD3 ubiquitination was observed with LPS or LPS with Polymyxin B treatment (Online Figure XIIA-B).

These experiments were repeated using primary mouse bone marrow monocytes. Similarly, β2M, but not TGFβ, induced SMAD3 ubiquitination (Figure 6B). SMAD4 ubiquitination was also determined in THP-1 cells. TGFβ decreased SMAD4 ubiquitination, while β2M induced an increase 24 hrs post-treatment (Figure 6D). Taken together, these data indicate that β2M and TGFβ signaling are ubiquitin ligase regulated; ubiquitin ligase activity is necessary for β2M signaling, but blocks TGFβ signaling.

DISCUSSION

Our data indicates that β2M and TGFβ signal and differentially polarize monocytes through a shared TGFβR dependent mechanism, but with divergent downstream signaling. β2M promotes an inflammatory monocyte phenotype in a SMAD-independent, non-canonical signaling dependent manner. Through both *in vitro* and *in vivo* studies, we showed that β2M increased the nuclear trafficking of transcription factors such as JNK and NFκB that regulate pro-inflammatory gene transcripts. Conversely, we showed that TGFβ promoted pro-reparative monocyte responses in a canonical TGFβR dependent signaling manner. TGFβ upregulated a master regulator of the pro-reparative phenotype, NR4A1 and promoted the nuclear translocation of SMAD2/3 and SMAD4 that act to increase pro-reparative transcripts.

Ubiquitin is a regulator of many receptor signaling pathways, including TGFβR signal transduction. However, it has not been prior shown to have a role in dictating monocyte phenotypes. Our data indicates that β2M promoted SMAD ubiquitination, which inhibited its nuclear translocation, and downregulated the SMAD-dependent canonical pathway. TGFβ decreased SMAD3 and SMAD4 ubiquitination and promoted the canonical pathway signaling. This suggests that even though β2M and TGFβ may each increase the phosphorylation of molecules in different signal transduction pathways, the ubiquitination state may be the major determinant of the downstream signaling and monocyte programing. It is interesting to note that inhibition of ubiquitin ligase activity alone increased monocyte *Il10,* perhaps demonstrating it to have an important role in maintaining basal monocyte immune differentiation as well. While our data is novel in highlighting how β2M and TGFβ dichotomously affect ubiquitin, it is unclear at the receptor level itself how β2M or TGFβ interact with the receptor to regulate ubiquitin ligase activity and which specific E3 ubiquitin ligases are responsible for the regulation of the canonical pathway. There is great redundancy in the E3 Ubiquitin ligases of both the canonical pathway (SMURF2, ROC1-SCFFbw1a, Ectodermin/Tif1γ)[21-23] and non-canonical pathway (TRAF6, XIAP)[16, 17, 27, 28] suggesting that there are likely multiple ligases responsible.

Our previous work showed that β2M and TGFβ are important for monocyte phenotype responses in the context of both acute myocardial infarction and aging[12, 34]. Our understanding of how monocytes change immune functions in the circulation and its impact on tissue injury and aging responses are poorly understood. Much of our knowledge comes from *in vitro* experiments and very few studies have characterized these phenomena *in vivo*. Because β2M and TGFβ plasma levels are changed in a wide variety of inflammatory and fibrotic diseases, we believe these findings are of broad importance and can be applied to many diseases. Anti-β2M and -TGFβ blocking therapies may not be effective ways to manage monocyte phenotypes as both proteins have numerous functions outside of monocyte signaling. β2M is a chaperone molecule for MHC I, HFE, and CD1[35], while TGFβ is a pluripotent growth factor that signals multiple cell types and is linked with ECM maintenance, cell survival/growth, and fibrosis. However, both proteins require dimer/multimerization to signal many different cell types, a potential means to target the function of each in the plasma[36-40]. Clarity in receptor signaling may also help in the development of future means to shift monocyte functions in a disease dependent manner.

SOURCES OF FUNDING
This work was supported by NIH/NHLBI grants HL141106-01A1 and HL142152 as well as AHA grant18CSA34020064 to C.N.M.

DISCLOSURES
No authors have any conflicts of interest.

SUPPLEMENTAL MATERIALS
Expanded Materials and Methods
Online Figures I – XII
Uncut blots

REFERENCES

1. Barbalat R, Lau L, Locksley RM and Barton GM. Toll-like receptor 2 on inflammatory monocytes induces type I interferon in response to viral but not bacterial ligands. *Nature immunology*. 2009;10:1200-7.
2. Serbina NV, Jia T, Hohl TM and Pamer EG. Monocyte-mediated defense against microbial pathogens. *Annual review of immunology*. 2008;26:421-52.
3. Hanna RN, Cekic C, Sag D, Tacke R, Thomas GD, Nowyhed H, Herrley E, Rasquinha N, McArdle S, Wu R, Peluso E, Metzger D, Ichinose H, Shaked I, Chodaczek G, Biswas SK and Hedrick CC. Patrolling monocytes control tumor metastasis to the lung. *Science (New York, NY)*. 2015;350:985-90.
4. Hilgendorf I, Gerhardt LM, Tan TC, Winter C, Holderried TA, Chousterman BG, Iwamoto Y, Liao R, Zirlik A, Scherer-Crosbie M, Hedrick CC, Libby P, Nahrendorf M, Weissleder R and Swirski FK. Ly-6Chigh monocytes depend on Nr4a1 to balance both inflammatory and reparative phases in the infarcted myocardium. *Circulation research*. 2014;114:1611-22.
5. Geissmann F, Jung S and Littman DR. Blood monocytes consist of two principal subsets with distinct migratory properties. *Immunity*. 2003;19:71-82.
6. Cros J, Cagnard N, Woollard K, Patey N, Zhang SY, Senechal B, Puel A, Biswas SK, Moshous D, Picard C, Jais JP, D'Cruz D, Casanova JL, Trouillet C and Geissmann F. Human CD14dim monocytes patrol and sense nucleic acids and viruses via TLR7 and TLR8 receptors. *Immunity*. 2010;33:375-86.
7. Wong KL, Tai JJ, Wong WC, Han H, Sem X, Yeap WH, Kourilsky P and Wong SC. Gene expression profiling reveals the defining features of the classical, intermediate, and nonclassical human monocyte subsets. *Blood*. 2011;118:e16-31.
8. Mills CD, Kincaid K, Alt JM, Heilman MJ and Hill AM. M-1/M-2 macrophages and the Th1/Th2 paradigm. *Journal of immunology (Baltimore, Md : 1950)*. 2000;164:6166-73.
9. Yang J, Zhang L, Yu C, Yang XF and Wang H. Monocyte and macrophage differentiation: circulation inflammatory monocyte as biomarker for inflammatory diseases. *Biomarker research*. 2014;2:1.
10. Xie J and Yi Q. Beta2-microglobulin as a potential initiator of inflammatory responses. *Trends in immunology*. 2003;24:228-9; author reply 229-30.
11. Zhang F, Wang H, Wang X, Jiang G, Liu H, Zhang G, Wang H, Fang R, Bu X, Cai S and Du J. TGF-beta induces M2-like macrophage polarization via SNAIL-mediated suppression of a pro-inflammatory phenotype. *Oncotarget*. 2016;7:52294-52306.

12. Hilt ZT, Pariser DN, Ture SK, Mohan A, Quijada P, Asante AA, Cameron SJ, Sterling JA, Merkel AR, Johanson AL, Jenkins JL, Small EM, McGrath KE, Palis J, Elliott MR and Morrell CN. Platelet-derived beta2M regulates monocyte inflammatory responses. *JCI Insight*. 2019;4.
13. Hilt ZT, Ture SK, Mohan A, Arne A and Morrell CN. Platelet-derived beta2m regulates age related monocyte/macrophage functions. *Aging (Albany NY)*. 2019;11:11955-11974.
14. Lo RS, Chen YG, Shi Y, Pavletich NP and Massague J. The L3 loop: a structural motif determining specific interactions between SMAD proteins and TGF-beta receptors. *The EMBO journal*. 1998;17:996-1005.
15. Wu RY, Zhang Y, Feng XH and Derynck R. Heteromeric and homomeric interactions correlate with signaling activity and functional cooperativity of Smad3 and Smad4/DPC4. *Molecular and cellular biology*. 1997;17:2521-8.
16. Yamashita M, Fatyol K, Jin C, Wang X, Liu Z and Zhang YE. TRAF6 mediates Smad-independent activation of JNK and p38 by TGF-beta. *Molecular cell*. 2008;31:918-24.
17. Hirata Y, Takahashi M, Morishita T, Noguchi T and Matsuzawa A. Post-Translational Modifications of the TAK1-TAB Complex. *International journal of molecular sciences*. 2017;18.
18. Freudlsperger C, Bian Y, Contag Wise S, Burnett J, Coupar J, Yang X, Chen Z and Van Waes C. TGF-beta and NF-kappaB signal pathway cross-talk is mediated through TAK1 and SMAD7 in a subset of head and neck cancers. *Oncogene*. 2013;32:1549-59.
19. Liu CP, Zhang X, Tan QL, Xu WX, Zhou CY, Luo M, Li X, Huang RY and Zeng X. NF-kappaB pathways are involved in M1 polarization of RAW 264.7 macrophage by polyporus polysaccharide in the tumor microenvironment. *PloS one*. 2017;12:e0188317.
20. Han MS, Jung DY, Morel C, Lakhani SA, Kim JK, Flavell RA and Davis RJ. JNK expression by macrophages promotes obesity-induced insulin resistance and inflammation. *Science (New York, NY)*. 2013;339:218-22.
21. Fukuchi M, Imamura T, Chiba T, Ebisawa T, Kawabata M, Tanaka K and Miyazono K. Ligand-dependent degradation of Smad3 by a ubiquitin ligase complex of ROC1 and associated proteins. *Molecular biology of the cell*. 2001;12:1431-43.
22. Dupont S, Mamidi A, Cordenonsi M, Montagner M, Zacchigna L, Adorno M, Martello G, Stinchfield MJ, Soligo S, Morsut L, Inui M, Moro S, Modena N, Argenton F, Newfeld SJ and Piccolo S. FAM/USP9x, a deubiquitinating enzyme essential for TGFbeta signaling, controls Smad4 monoubiquitination. *Cell*. 2009;136:123-35.
23. Lin X, Liang M and Feng XH. Smurf2 is a ubiquitin E3 ligase mediating proteasome-dependent degradation of Smad2 in transforming growth factor-beta signaling. *The Journal of biological chemistry*. 2000;275:36818-22.
24. Salabei JK, Cummins TD, Singh M, Jones SP, Bhatnagar A and Hill BG. PDGF-mediated autophagy regulates vascular smooth muscle cell phenotype and resistance to oxidative stress. *The Biochemical journal*. 2013;451:375-88.
25. Mockel M, Muller R, Searle J, Slagman A, De Bruyne B, Serruys P, Weisz G, Xu K, Holert F, Muller C, Maehara A and Stone GW. Usefulness of Beta2-Microglobulin as a Predictor of All-Cause and Nonculprit Lesion-Related Cardiovascular Events in Acute Coronary Syndromes (from the PROSPECT Study). *The American journal of cardiology*. 2015;116:1034-40.
26. Chen Y, Kam CS, Liu FQ, Liu Y, Lui VC, Lamb JR and Tam PK. LPS-induced up-regulation of TGF-beta receptor 1 is associated with TNF-alpha expression in human monocyte-derived macrophages. *Journal of leukocyte biology*. 2008;83:1165-73.
27. Mu Y, Gudey SK and Landstrom M. Non-Smad signaling pathways. *Cell and tissue research*. 2012;347:11-20.
28. Gudey SK and Landstrom M. The Role of Ubiquitination to Determine Non-Smad Signaling Responses. *Methods in molecular biology (Clifton, NJ)*. 2016;1344:355-63.
29. Inoue Y and Imamura T. Regulation of TGF-beta family signaling by E3 ubiquitin ligases. *Cancer science*. 2008;99:2107-12.

30. De Boeck M and ten Dijke P. Key role for ubiquitin protein modification in TGFbeta signal transduction. *Upsala journal of medical sciences*. 2012;117:153-65.
31. Mund T, Lewis MJ, Maslen S and Pelham HR. Peptide and small molecule inhibitors of HECT-type ubiquitin ligases. *Proceedings of the National Academy of Sciences of the United States of America*. 2014;111:16736-41.
32. Xie F, Zhang Z, van Dam H, Zhang L and Zhou F. Regulation of TGF-beta Superfamily Signaling by SMAD Mono-Ubiquitination. *Cells*. 2014;3:981-93.
33. Hull C, McLean G, Wong F, Duriez PJ and Karsan A. Lipopolysaccharide signals an endothelial apoptosis pathway through TNF receptor-associated factor 6-mediated activation of c-Jun NH2-terminal kinase. *Journal of immunology (Baltimore, Md : 1950)*. 2002;169:2611-8.
34. Hilt ZT, Ture SK, Mohan A, Arne A and Morrell CN. Platelet-derived beta2m regulates age related monocyte/macrophage functions. *Aging*. 2019;11.
35. Li L, Dong M and Wang XG. The Implication and Significance of Beta 2 Microglobulin: A Conservative Multifunctional Regulator. *Chinese medical journal*. 2016;129:448-55.
36. Hall Z, Schmidt C and Politis A. Uncovering the Early Assembly Mechanism for Amyloidogenic beta2-Microglobulin Using Cross-linking and Native Mass Spectrometry. *The Journal of biological chemistry*. 2016;291:4626-37.
37. Nomura T, Huang WC, Zhau HE, Josson S, Mimata H and Chung LW. beta2-Microglobulin-mediated signaling as a target for cancer therapy. *Anti-cancer agents in medicinal chemistry*. 2014;14:343-52.
38. Estacio SG, Krobath H, Vila-Vicosa D, Machuqueiro M, Shakhnovich EI and Faisca PF. A simulated intermediate state for folding and aggregation provides insights into DeltaN6 beta2-microglobulin amyloidogenic behavior. *PLoS computational biology*. 2014;10:e1003606.
39. Grainger DJ, Wakefield L, Bethell HW, Farndale RW and Metcalfe JC. Release and activation of platelet latent TGF-beta in blood clots during dissolution with plasmin. *Nature medicine*. 1995;1:932-7.
40. Shi M, Zhu J, Wang R, Chen X, Mi L, Walz T and Springer TA. Latent TGF-beta structure and activation. *Nature*. 2011;474:343-9.

FIGURE LEGENDS

Figure 1. Increased plasma β2M promoted a pro-inflammatory monocyte phenotype *in vivo*. WT and Plt-β2M$^{-/-}$ mice were treated with β2M i.v. for 3d and on d4 monocyte phenotypes were determined by flow cytometry and qRT-PCR. A) β2M treatment increased circulating monocyte Ly6C and *Cxcl1* in both WT and Plt-β2M$^{-/-}$ mice (N=5 WT, N=4 Plt-β2M$^{-/-}$, mean ± SEM, *P<0.05, **P<0.01, one-way ANOVA with Bonferroni correction). B) β2M decreased markers reparative monocyte differentiation including *Il27*, *Il10*, *Nr4a1* (N=3, mean ± SD, *P<0.05, **P<0.01, one-way ANOVA with Bonferroni correction). C) Whole blood monocytes from WT and Plt-β2M$^{-/-}$ mice treated with β2M had decreased pSMAD2/3 nuclear localization determined by imaging flow cytometry. Representative images of monocytes shown. Quantified images were pooled from 4 WT mice and 5 Plt-β2M$^{-/-}$ mice (mean ± SEM, **P<0.01, one-way ANOVA with Bonferroni correction).

Figure 2. Increased plasma TGFβ promoted a reparative monocyte phenotype *in vivo*. WT and Plt-β2M$^{-/-}$ mice were treated with TGFβ i.v. for 3d and on d4 monocyte phenotypes determined. A) TGFβ decreased monocyte Ly6C (N=5, mean ± SEM, *P<0.05, **P<0.01, one-way ANOVA with Bonferroni correction) and B) increased markers of reparative monocyte phenotype, including *Arg1, Chil3* and *Vegfa,* particularly in Plt-β2M$^{-/-}$ mice (N=3, mean ± SD, *P<0.05, **P<0.01, one-way ANOVA with Bonferroni correction). C) Mice treated i.v. with β2M, but not TGFβ, had increased plasma KC in WT and Plt-β2M$^{-/-}$ mice (N=16 WT D0, N=15 WT D4 β2M, N=10 WT D4 TGFβ, N=14 Plt-β2M$^{-/-}$ D0, N=11 Plt-β2M$^{-/-}$ D4, mean ± SE, *P<0.05, one-way ANOVA with Bonferroni correction). D) TGFβ increased pSMAD2/3 and NR4A1 nuclear localization and E) decreased pJNK and NFkB nuclear localization. Representative images of monocytes shown. Quantified images were pooled from 5 mice (mean ± SEM, **P<0.01, one-way ANOVA with Bonferroni correction).

Figure 3. TGFβR inhibitor blocked the *in vivo* effects of both β2M and TGFβ. Mice were treated with DMSO, β2M, or TGFβ, ± SB431542, i.v. for 3d and on d4 monocyte phenotypes were determined. A) β2M increased *Cxcl1*, while TGFβ increased *Il27,* that were both decreased by TGFβR inhibitor treatment (N=3, mean ± SD, *P<0.05, **P<0.01, one-way ANOVA with Bonferroni correction). SB431542 blocked TGFβ induced B) SMAD4 and C) NR4A1 nuclear localization and D) attenuated β2M induced pJNK nuclear trafficking. Representative images of monocytes. Quantified images were pooled from 5 mice (mean ± SEM, *P<0.05, **P<0.01, one-way ANOVA with Bonferroni correction).

Figure 4. TGFβ and β2M induced different transcription factor nuclear trafficking *in vitro*. A-B) THP-1 cells were treated with β2M or TGFβ. In a time-course dependent manner nuclear A) NFkB or B) SMAD3 were determined by immunoblot. C-G) Imaging flow cytometry was performed for C) pJNK, D) pSMAD2/3, or E) SMAD4. F-G) As a tertiary method of confirmation nuclear localization of F) pJNK and G) SMAD4 was confirmed through confocal microscopy (scale bar, 5 μm). H) Platelet releasate increased pJNK and decreased SMAD nuclear localization that was limited by anti-β2M antibody. Representative images of monocytes shown. Quantified images were pooled from 4 independent treatment replicates (mean ± SEM, *P<0.05, **P<0.01, one-way ANOVA with Bonferroni correction). I) Mouse monocytes were treated with β2M or TGFβ and at multiple time points inflammatory markers *Cxcl8, Tnf*, and *Mmp9* or reparative markers *Timp1, Arg1* or *Il10* were quantified by qRT-PCR (N=3, mean ± SEM, *P<0.05, **P<0.01, one-way ANOVA with Bonferroni correction).

Figure 5. β2M signaling is ubiquitin ligase dependent. Ubiquitin ligase inhibitor blocked β2M induced inflammatory, and increased TGFβ induced reparative monocyte phenotypes. THP-1s were treated with Heclin and β2M or TGFβ. A) CD16^{+} surface expression and B) gene expression were determined 24 hrs later by FACS and qRT-PCR respectively (N=4, mean ± SEM, *P<0.05, **P<0.01, one-way ANOVA with Bonferroni correction).

Figure 6. β2M induced SMAD ubiquitination. A and C) RAW 264.7 macrophages, B) primary mouse monocytes, or D) THP-1s were treated with TGFβ or β2M. At multiple time points SMAD3 and SMAD4 were immunoprecipitated and its ubiquitination determined by immunoblot. β2M but not TGFβ increased SMAD ubiquitination.

NOVELTY AND SIGNIFICANCE

What Is Known?

- Monocytes polarize towards pro-inflammatory or pro-reparative depending on the immune environment.
- Platelet-derived Beta-2 microglobulin (β2M) and transforming growth factor beta (TGFβ) act as ligands through a shared monocyte receptor.

What New Information Does This Article Contribute?

- *In vivo* demonstration of acute plasma β2M and TGFβ effects on monocyte signal transduction pathways.
- β2M promotes SMAD ubiquitination and non-canonical signal transduction in monocytes.
- TGFβ promotes the canonical signal transduction pathway in monocytes.

Monocytes can be polarized as either pro-inflammatory or pro-reparative, but the *in vivo* molecular mechanisms are not well described. We now show that TGFβ promotes a pro-reparative monocyte phenotype through canonical signal transduction, while β2M promotes a pro-inflammatory monocyte phenotype through a non-canonical signal transduction pathway. Platelet-derived β2M-mediated molecular signaling pathways are dependent on the ubiquitination of SMAD proteins that prevents their translocation into the nucleus. These new insights into the molecular control of the signal transduction pathways may lead to novel means to modulate monocyte phenotype in disease states.

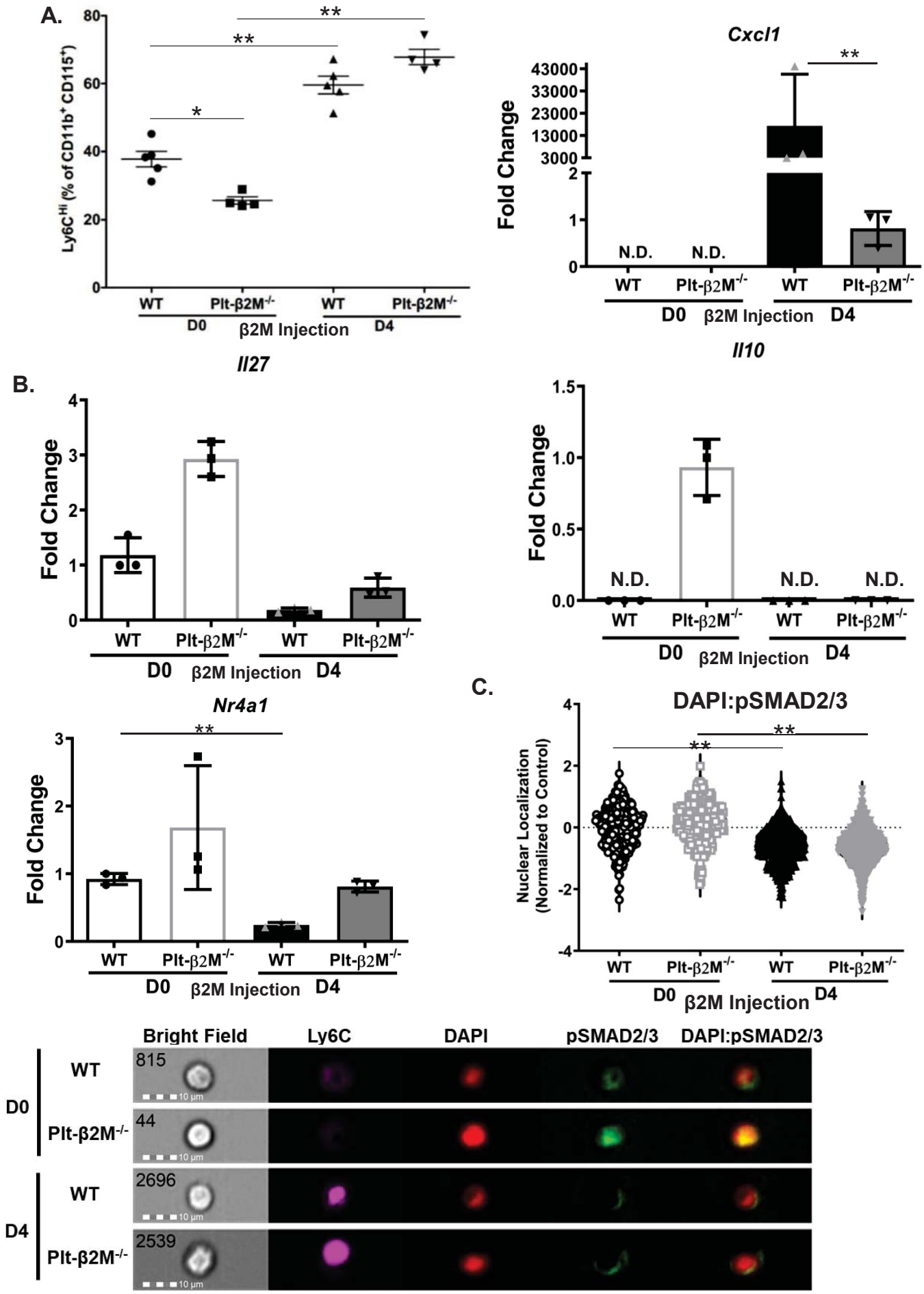
A.
Ly6C^Hi (% of CD11b+ CD115+)
WT
Plt-β2M-/-
WT
Plt-β2M-/-
D0
β2M Injection
D4
Cxcl1
Fold Change
N.D.
N.D.
D0 β2M Injection D4
B.
Il27
Fold Change
D0 β2M Injection D4
Il10
Fold Change
N.D.
N.D.
N.D.
D0 β2M Injection D4
Nr4a1
Fold Change
D0 β2M Injection D4
C.
DAPI:pSMAD2/3
Nuclear Localization (Normalized to Control)
D0 β2M Injection D4
Bright Field
Ly6C
DAPI
pSMAD2/3
DAPI:pSMAD2/3
D0
WT
Plt-β2M-/-
D4
WT
Plt-β2M-/-
815
44
2696
2539
10 μm

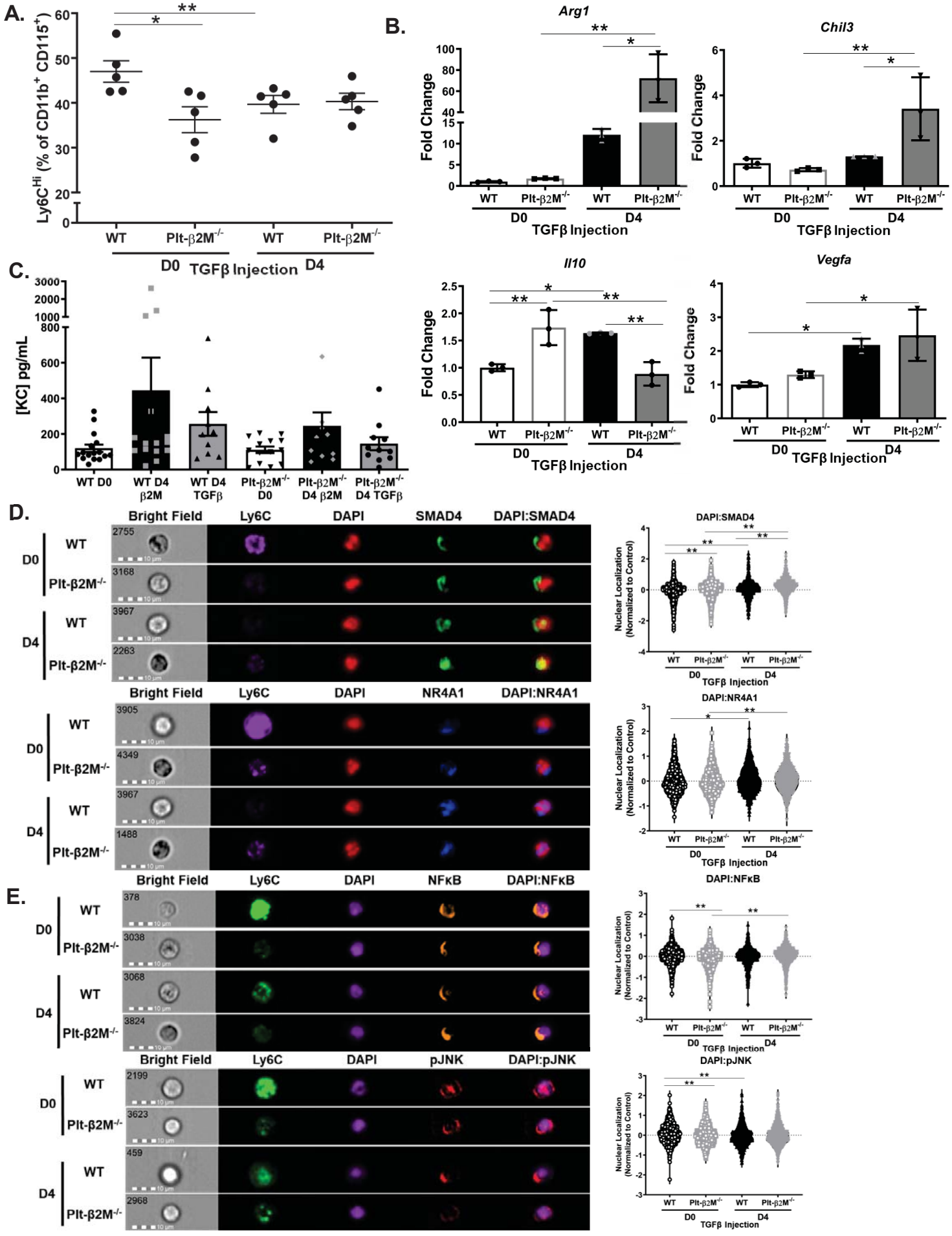
A.
Ly6C^Hi (% of CD11b+ CD115+)
WT
Plt-β2M-/-
WT
Plt-β2M-/-
D0
TGFβ Injection
D4
B.
Arg1
Chil3
Fold Change
WT
Plt-β2M-/-
WT
Plt-β2M-/-
D0
D4
TGFβ Injection
C.
[KC] pg/mL
WT D0
WT D4 β2M
WT D4 TGFβ
Plt-β2M-/- D0
Plt-β2M-/- D4 β2M
Plt-β2M-/- D4 TGFβ
Il10
Vegfa
D.
Bright Field
Ly6C
DAPI
SMAD4
DAPI:SMAD4
NR4A1
DAPI:NR4A1
Nuclear Localization (Normalized to Control)
E.
NFκB
DAPI:NFκB
pJNK
DAPI:pJNK

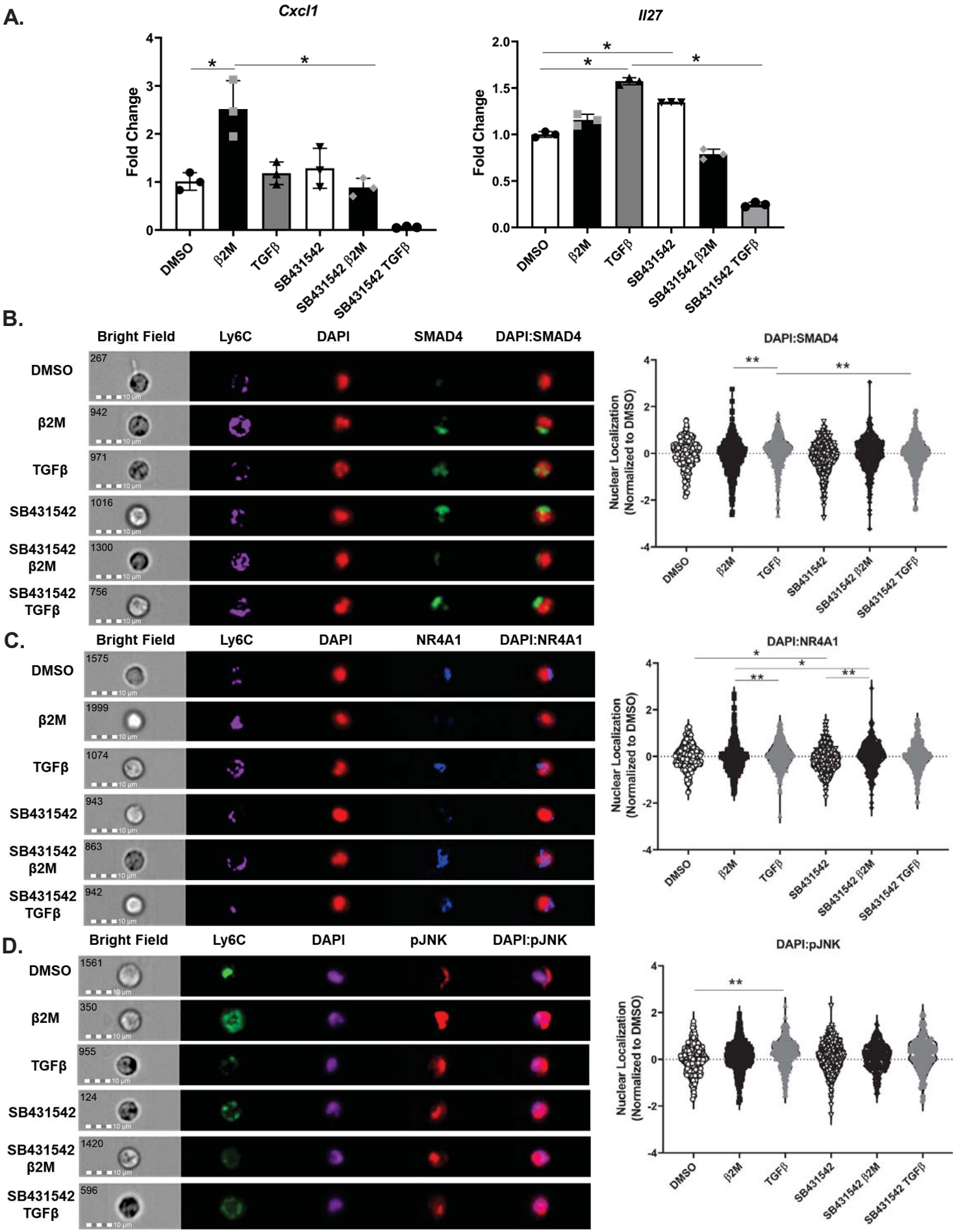
A.
Cxcl1
Il27
Fold Change
DMSO
β2M
TGFβ
SB431542
SB431542 β2M
SB431542 TGFβ
B.
Bright Field
Ly6C
DAPI
SMAD4
DAPI:SMAD4
Nuclear Localization (Normalized to DMSO)
C.
NR4A1
DAPI:NR4A1
D.
pJNK
DAPI:pJNK

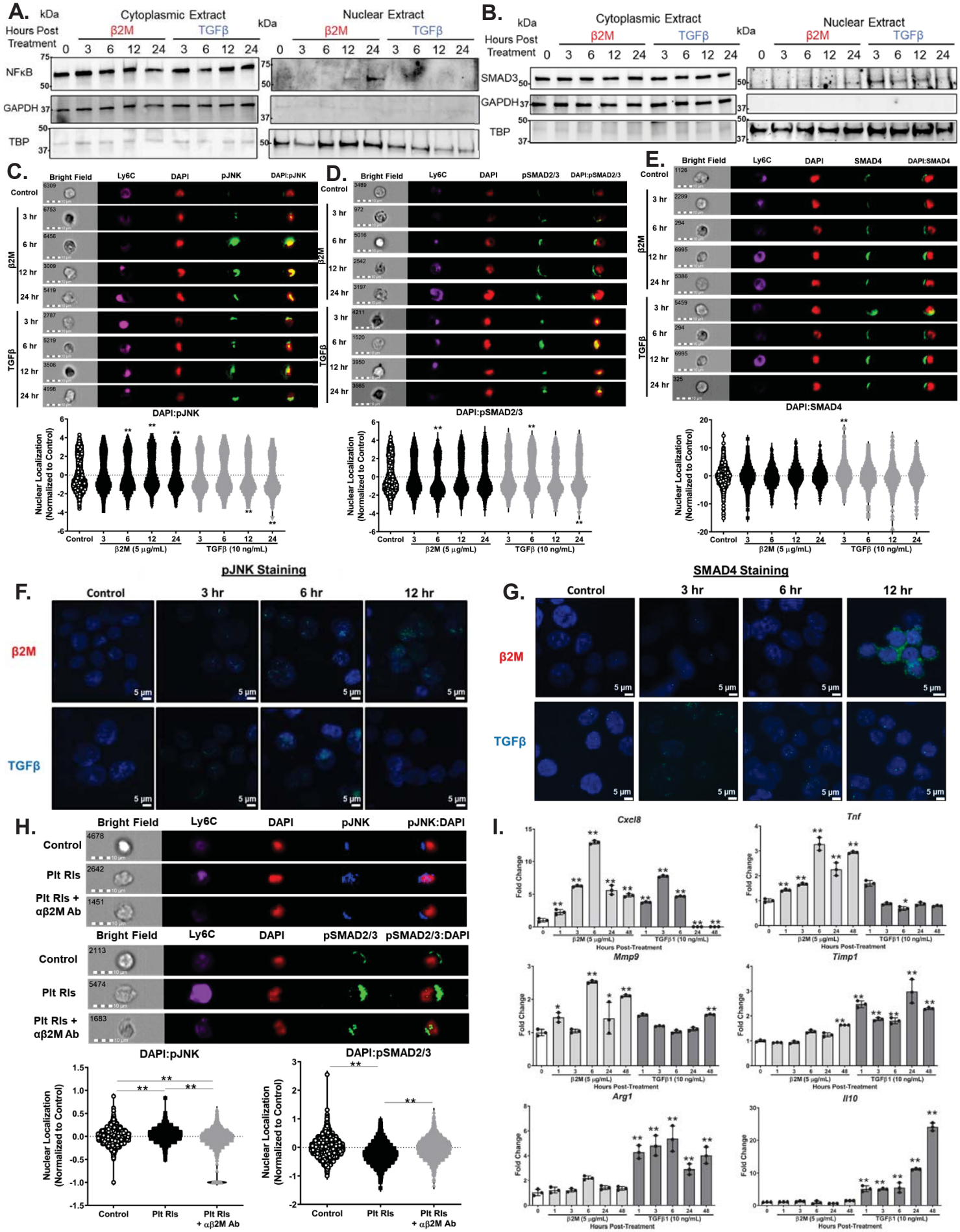
A.
Cytoplasmic Extract
Nuclear Extract
β2M
TGFβ
Hours Post Treatment
NFκB
GAPDH
TBP
B.
SMAD3
C.
Bright Field
Ly6C
DAPI
pJNK
DAPI:pJNK
D.
pSMAD2/3
DAPI:pSMAD2/3
E.
SMAD4
DAPI:SMAD4
Nuclear Localization (Normalized to Control)
β2M (5 μg/mL)
TGFβ (10 ng/mL)
pJNK Staining
SMAD4 Staining
F.
G.
Control
3 hr
6 hr
12 hr
5 μm
H.
pJNK:DAPI
pSMAD2/3:DAPI
Plt RIs
Plt RIs + αβ2M Ab
I.
Cxcl8
Tnf
Mmp9
Timp1
Arg1
Il10
Fold Change
Hours Post-Treatment

FIGURE 5

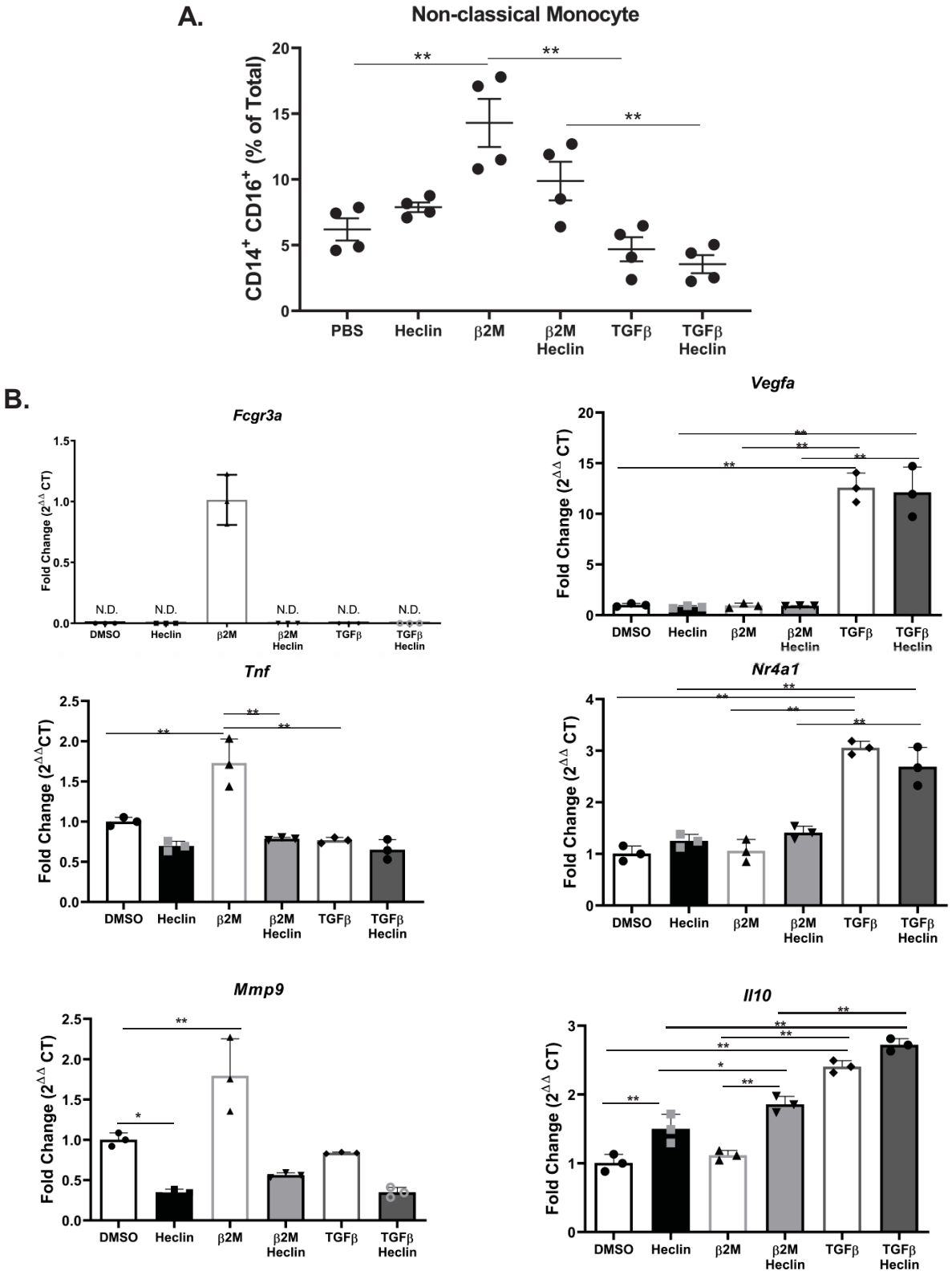
A.
Non-classical Monocyte
CD14+ CD16+ (% of Total)
PBS
Heclin
β2M
β2M Heclin
TGFβ
TGFβ Heclin
B.
Fcgr3a
Fold Change (2ΔΔ CT)
N.D.
DMSO
Heclin
β2M
β2M Heclin
TGFβ
TGFβ Heclin
Vegfa
Tnf
Nr4a1
Mmp9
Il10

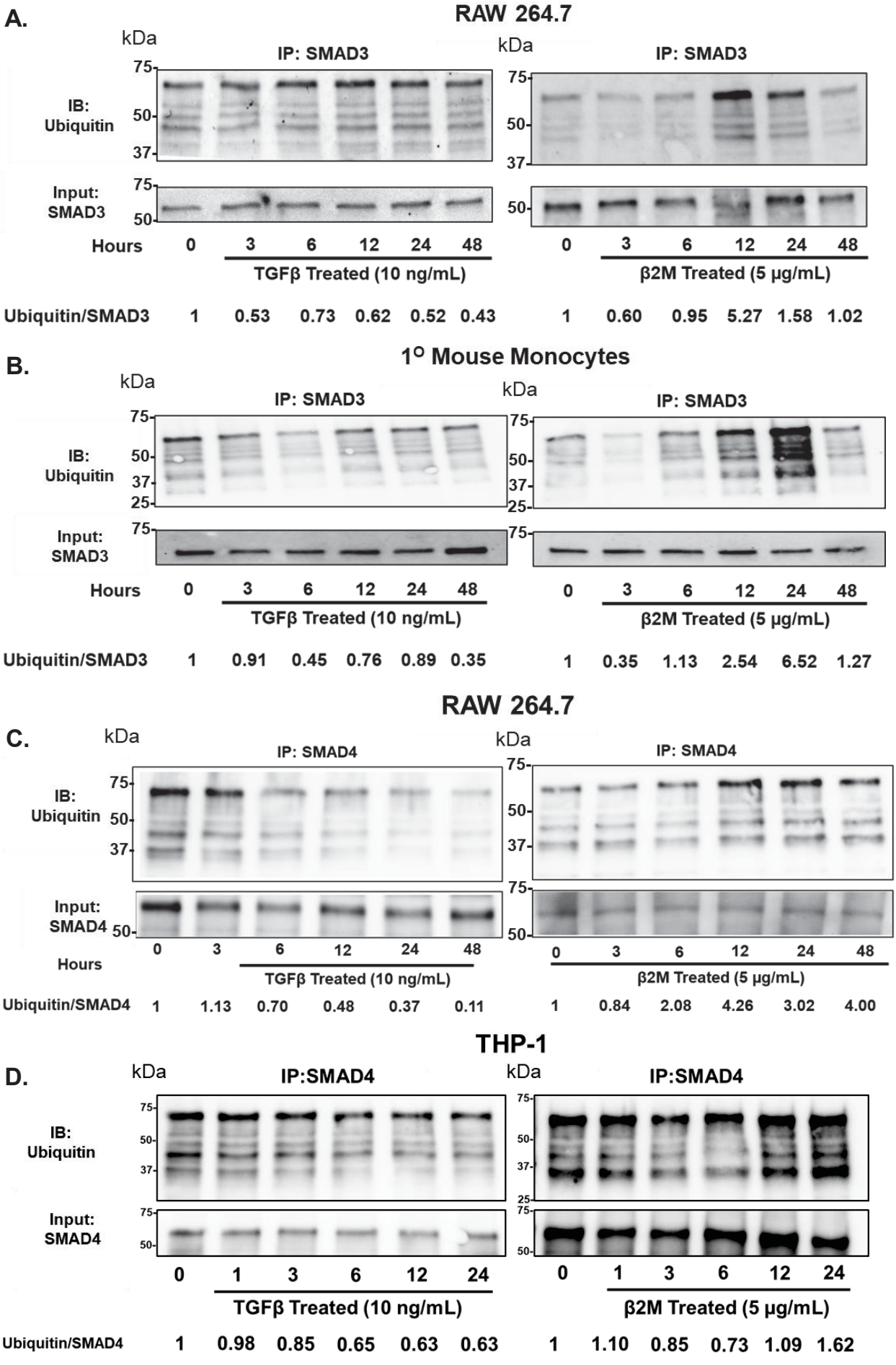
A.
RAW 264.7
kDa
IP: SMAD3
IB: Ubiquitin
Input: SMAD3
75
50
37
Hours 0 3 6 12 24 48
TGFβ Treated (10 ng/mL)
β2M Treated (5 μg/mL)
Ubiquitin/SMAD3 1 0.53 0.73 0.62 0.52 0.43
1 0.60 0.95 5.27 1.58 1.02
B.
1° Mouse Monocytes
25
Ubiquitin/SMAD3 1 0.91 0.45 0.76 0.89 0.35
1 0.35 1.13 2.54 6.52 1.27
C.
RAW 264.7
IP: SMAD4
Input: SMAD4
Ubiquitin/SMAD4 1 1.13 0.70 0.48 0.37 0.11
1 0.84 2.08 4.26 3.02 4.00
D.
THP-1
0 1 3 6 12 24
Ubiquitin/SMAD4 1 0.98 0.85 0.65 0.63 0.63
1 1.10 0.85 0.73 1.09 1.62